14-3-3σ regulates B-cell homeostasis through stabilization of FOXO1

Yu-Wen Su[a,b], Zhenyue Hao[a], Atsushi Hirao[a,c], Kazuo Yamamoto[a], Wen-Jye Lin[a], Ashley Young[a], Gordon S. Duncan[a], Hiroki Yoshida[a,d], Andrew Wakeham[a], Philipp A. Lang[a], Kiichi Murakami[a], Heiko Hermeking[e], Bert Vogelstein[f], Pamela Ohashi[a], and Tak W. Mak[a,1]

[a]Campbell Family Cancer Research Institute, Ontario Cancer Institute, University Health Network, Toronto, ON, Canada M5G 2C1; [b]Department of Immunology Research Center, National Health Research Institute, Zhunan 35053, Taiwan; [c]Division of Molecular Genetics, Center for Cancer and Stem Cell Research, Cancer Research Institute, Kanazawa University, Kanazawa 920-0934, Japan; [d]Department of Biomolecular Sciences, Faculty of Medicine, Saga University, Nabeshima, Saga 849-8501, Japan; [e]Experimental and Molecular Pathology, Institute of Pathology, Ludwig-Maximilians-University, D-80337 Munich, Germany; and [f]Sidney Kimmel Comprehensive Cancer Center, Baltimore, MD 21231

Contributed by Tak W. Mak, November 25, 2010 (sent for review October 7, 2010)

14-3-3σ regulates cytokinesis and cell cycle arrest induced by DNA damage but its role in the immune system is unknown. Using gene-targeted 14-3-3σ–deficient (i.e., KO) mice, we studied the role of 14-3-3σ in B-cell functions. Total numbers of B cells were reduced by spontaneous apoptosis of peripheral B cells. Upon B-cell antigen receptor engagement in vitro, KO B cells did not proliferate properly or up-regulate CD86. In response to T cell-independent antigens, KO B cells showed poor secretion of antigen-specific IgM. This deficit led to increased lethality of KO mice after vesicular stomatitis virus infection. KO B cells showed elevated total FOXO transcriptional activity but also increased FOXO1 degradation. Coimmunoprecipitation revealed that endogenous 14-3-3σ protein formed a complex with FOXO1 protein. Our results suggest that 14-3-3σ maintains FOXO1 at a consistent level critical for normal B-cell antigen receptor signaling and B-cell survival.

The seven members of the 14-3-3 family (β, ε, γ, η, τ, ζ, and σ) are conserved acidic proteins expressed in all mammalian cells (1–3). As molecular scaffolds, the 14-3-3 proteins affect many aspects of cellular physiology, including cell survival, proliferation, differentiation, and intracellular signaling (4). This article focuses on 14-3-3σ (also called stratifin or SFN), a cell cycle inhibitor induced by p53 in response to DNA damage. 14-3-3σ inhibits cell cycle entry by sequestering Cdc2 in the cytoplasm (5, 6) and controls mitosis by influencing translation (7).

During B-cell development, immature B cells expressing the B-cell antigen receptor (BCR) leave the bone marrow (BM), migrate to the spleen or periphery, and differentiate into follicular (FO) or marginal zone (MZ) mature B cells. FO B cells, which localize to the lymphoid follicles of the spleen and lymph nodes, mainly participate in T cell-dependent (TD) immune responses (8). With help from $CD4^+$ T cells, antigen-specific FO B cells undergo the selective expansion and further differentiate to plasma cells with the capacity to secrete Abs. In contrast, MZ B cells reside primarily around the periphery of splenic lymphoid nodules, capturing blood-borne antigens and responding to T cell-independent (TI) antigens (8). Signaling essential for B-cell survival and differentiation is mediated through the BCR (9, 10). BCR engagement activates the PI3K signaling cascade, which culminates in Akt/PKB activation (11). Activated Akt phosphorylates numerous protein substrates, including the Forkhead family of transcription factor FOXO subfamily, that regulate apoptosis, oxidative response, DNA repair, cell-cycle arrest, differentiation, metabolism, and longevity (12–14). Of the four known FOXO members—FOXO1 (FKHR), FOXO3a (FKHRL1), FOXO4 (AFX), and FOXO6—only FOXO1 and FOXO3a play a critical role for B-cell physiology (15, 16). In non–B-cell lines, phosphorylation (P) of FOXO by Akt on T24 and S256 provides docking sites for 14-3-3 proteins, and 14-3-3 docking is required for the nuclear export (inactivation) of P-FOXO (17, 18). Disruption of 14-3-3/P-FOXO interaction leads to FOXO-dependent apoptosis, suggesting that 14-3-3 proteins integrate prosurvival signals by suppressing FOXO-mediated apoptosis (19, 20).

Here we show that gene-targeted disruption of 14-3-3σ in mice impairs B-cell homeostasis as a result of enhanced apoptosis of peripheral B cells. Loss of 14-3-3σ led to abnormal BCR signaling that damaged the TI immune response; inhibition of early antigen-specific IgM secretion; increased degradation of FOXO1 protein; and elevated FOXOs transcriptional activity. Thus, 14-3-3σ is essential for B-cell homeostasis because it maintains steady-state FOXO1 protein and modulates FOXO-mediated apoptosis.

Results

Generation of 14-3-3σ–Deficient Mice. We first used quantitative real-time PCR (qRT-PCR) to analyze 14-3-3σ in B-cell subsets from WT mice. 14-3-3σ mRNA was relatively high in FO and recirculating B cells but relatively low in other B-cell subsets (Fig. S1*A*), implying a requirement for 14-3-3σ in mature B cells. We then generated 14-3-3σ–deficient (i.e., KO) mice by conventional gene targeting (Fig. S1 *B* and *C*). Northern blotting of mRNA from WT and KO ES cells that were subjected to 10-Gy irradiation confirmed that 14-3-3σ mRNA could not be induced in KO cells (Fig. S1*D*). Loss of 14-3-3σ protein in cells from untreated KO mice was verified by Western blotting (Fig. S1*E*). KO mice were born at the expected Mendelian ratio, and were viable and fertile.

B-Cell Homeostasis. Examination of B-cell subsets in the BM by flow cytometry (FACS) analysis revealed that early B-cell development in KO mice was largely normal (Fig. 1*A* and Fig. S2*A*) but that recirculating B cells were drastically reduced (3.1% for KO vs. 14.2% for WT; Fig. 1*B* and Table 1). There was also a maturation defect in the mutants, as the total number of splenic B cells in KO mice was only one third of the WT, and both FO and MZ B cells were greatly decreased (Fig. 1 *C* and *D* and Table 1). The cellularity of splenic immature B cells was similar in WT and KO mice (Fig. 1*C* and Table 1). Surface levels of IgM and IgD on KO splenic B cells were normal but CD21 was significantly lower (Fig. 1*E*). Last, IgM^+CD5^+ B1a peritoneal B cells were reduced in KO mice (Fig. 1*F*).

We next used immunohistochemistry (IHC) to explore splenic microarchitecture. Staining of WT spleen sections with anti-CD3ε and anti-B220 revealed T cells in the periarteriolar lymphoid sheath, and B cells clustered outside of the periarteriolar lymphoid sheath around the T-cell zone (Fig. 1*G*, *Left*). In

Author contributions: Y.-W.S. and T.W.M. designed research; Y.-W.S., Z.H., A.H., K.Y., W.-J.L., A.Y., G.S.D., H.Y., A.W., P.A.L., and K.M. performed research; H.H., B.V., P.O., and T.W.M. contributed new reagents/analytic tools; Y.-W.S. and Z.H. analyzed data; and Y.-W.S. and T.W.M. wrote the paper.

The authors declare no conflict of interest.

Freely available online through the PNAS open access option.

[1]To whom correspondence should be addressed. E-mail: tmak@uhnres.utoronto.ca.

This article contains supporting information online at www.pnas.org/lookup/suppl/doi:10.1073/pnas.1017729108/-/DCSupplemental.

IMMUNOLOGY

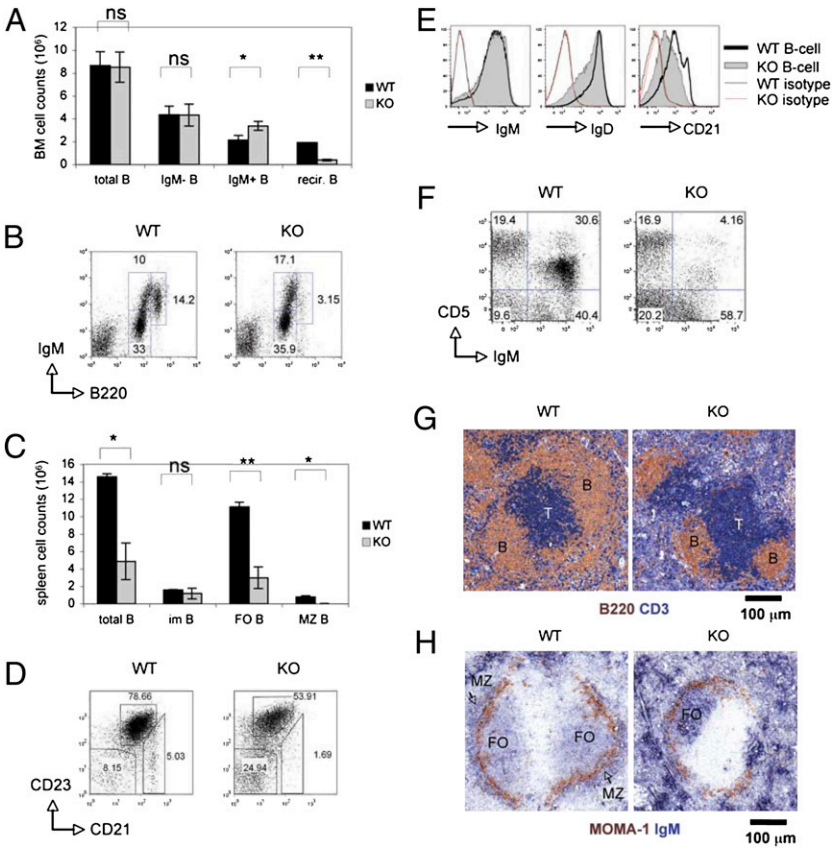

Fig. 1. B-cell maturation. (*A* and *B*) Decreased recirculating B cells. (*A*) BM cellularity histogram shows total B220$^+$ B cells (total B), B220$^+$IgM$^-$ B-cell progenitors (IgM$^-$ B), B220^{low}IgM$^+$ immature B cells (IgM$^+$ B), and B220^{high}IgM$^+$ recirculating B cells (recir. B). For all figures, data are the mean ± SD of triplicates and/or represent two to three independent trials (*$P < 0.05$; **$P < 0.005$; ns, not significant). All data were collected from mice of 8 and 16 wk. (*B*) FACS of IgM versus B220 by the cells in *A*. For all FACS profiles, data reflect the gating of 10,000 lymphocytes. Numbers are percentages of B220$^+$IgM$^-$ progenitor, B220^{low}IgM$^+$ immature and B220^{high}IgM$^+$ recirculating B cells. (*C* and *D*) Decreased splenic B cells. (*C*) Splenic cellularity histogram showing total B220$^+$ B cells (total B), B220$^+$CD21$^-$CD23$^-$ immature B cells (im B), B220$^+$CD21^{low}CD23^{high} FO B cells (FO B), and B220$^+$CD21^{high}CD23^{low} MZ B cells (MZ B). (*D*) FACS of CD23 versus CD21 of the cells in *C*. Numbers are percentages of CD21$^-$CD23$^-$ immature B cells, CD21^{low}CD23^{high} FO B cells, and CD21^{high}CD23^{low} MZ B cells. (*E*) Decreased CD21 expression. FACS of B-cell IgM, IgD, and CD21 expression. (*F*) Reduced peritoneal B cells. FACS of CD5 versus IgM by peritoneal B cells. (*G* and *H*) Altered splenic microarchitecture. (*G*) IHC staining of spleens with anti-B220 (brown) plus anti-CD3ε (blue). (*H*) IHC staining of spleens with anti–MOMA-1 (brown) plus anti-IgM (blue).

contrast, the B-cell zone was much smaller in KO mice and the T-cell zone was not consistently surrounded by B cells (Fig. 1*G*, *Right*). Staining of WT spleen sections with anti-metallophilic macrophage (MOMA-1) Ab showed the expected ring structure of the marginal sinus, with FO B cells inside the sinus and MZ B cells outside it (Fig. 1*H*, *Left*). However, anti–MOMA-1 staining of KO spleens revealed that the FO B-cell area was significantly smaller than in the WT, and the MZ B-cell area was absent (Fig. 1*H*, *Right*). These findings are consistent with our FACS data and confirm that peripheral B cells are severely reduced in mice lacking 14-3-3σ.

The observed defect in B-cell maturation could be caused by an inherent B-cell defect or altered stromal signaling. We therefore adoptively transferred WT or KO BM cells into γ-irradiated RAG1$^{-/-}$ or μMT mice, and analyzed mature B-cell subsets in the reconstituted chimeras at 8 wk after transfer. Mice that received KO BM cells showed a reduction in FO B cells and the absence of MZ B cells in their spleens (Fig. S2 *B* and *C*). Thus, the defect in B-cell homeostasis that occurs in the absence of 14-3-3σ is B-cell–intrinsic.

Table 1. Cellularity of B-cell subsets in WT and 14-3-3σ–deficient (i.e., KO) mice

Subset	Cellularity			
BM	Total	IgM$^-$	IgM$^+$	Recirculating
WT	8.6 ± 1.1	4.3 ± 0.7	2.1 ± 0.4	1.92 ± 0.01
KO	8.5 ± 1.3	4.3 ± 0.9	3.3 ± 0.3	0.39 ± 0.06
Spleen*	Total	imm†	FO	MZ
WT	14.5 ± 0.3	1.6 ± 0.07	11.1 ± 0.5	0.8 ± 0.14
KO	4.8 ± 2.1	1.18 ± 0.6	3.0 ± 1.2	0.01 ± 0.005

Total B220$^+$ B cells (total) from BM were immunostained and fractionated by FACS into subsets: B220$^+$IgM$^-$ B-cell progenitors (IgM$^-$), B220^{low}IgM$^+$ immature B cells (IgM$^+$), and B220^{high}IgM$^+$ recirculating B cells. Values shown are absolute cell numbers (×10^{-6}).

*Total splenic B220$^+$ B cells (total) were immunostained and fractionated by FACS into subsets: CD21$^-$CD23$^-$ immature B cells (imm), CD21^{low}CD23^{high} FO B cells (FO), and CD21^{high}CD23^{low} MZ B cells (MZ).

†imm, immature.

B-Cell Apoptosis, Homeostatic Expansion, and BCR-Stimulated Proliferation. To dissect the molecular mechanism whereby 14-3-3σ contributes to B-cell homeostasis, we first asked whether 14-3-3σ deficiency affected B-cell survival. Staining of splenocytes with Annexin V plus propidium iodide (PI) revealed that 3.4% of B220$^+$ B cells were apoptotic in WT mice, whereas 15.8% of KO B cells were dying (Fig. 2*A*). This elevated apoptosis was B-cell–intrinsic, as increased spontaneous apoptosis was also found in RAG1$^{-/-}$/KO chimeras (Fig. S3*A*). Because BCR engagement in the absence of T-cell help can accelerate B-cell apoptosis (21), we investigated the role of 14-3-3σ in BCR-mediated apoptosis ex vivo. Stimulation of isolated WT B cells for 24 h with 5 μg/mL anti-IgM led to a reduction in viable B cells (7AAD$^-$) from 100% to 75%, whereas stimulated KO B cells were only 50% viable (Fig. 2*B*). Thus, 14-3-3σ is required for splenic B-cell survival and inhibition of BCR-mediated apoptosis.

We next asked whether loss of 14-3-3σ influenced B-cell proliferation in vivo. WT and KO mice were fed BrdU-containing drinking water for 3 d and splenic B cells were analyzed by intracellular staining with anti-BrdU plus 7AAD followed by FACS. In WT mice, the proportion of BrdU$^+$ B cells (G1/S phases) was 9.4%; in contrast, BrdU$^+$ B cells represented 14.9% of total splenic B cells in KO mice, indicating increased B-cell proliferation (Fig. 2*C*). IHC study of spleen sections using anti-B220 plus anti-Ki67 confirmed that proliferating Ki67$^+$B220$^+$ splenocytes were dramatically increased in KO mice (Fig. S3*B*). Thus, in the absence of 14-3-3σ, the proportion of B cells that undergoes proliferation in vivo is abnormally high.

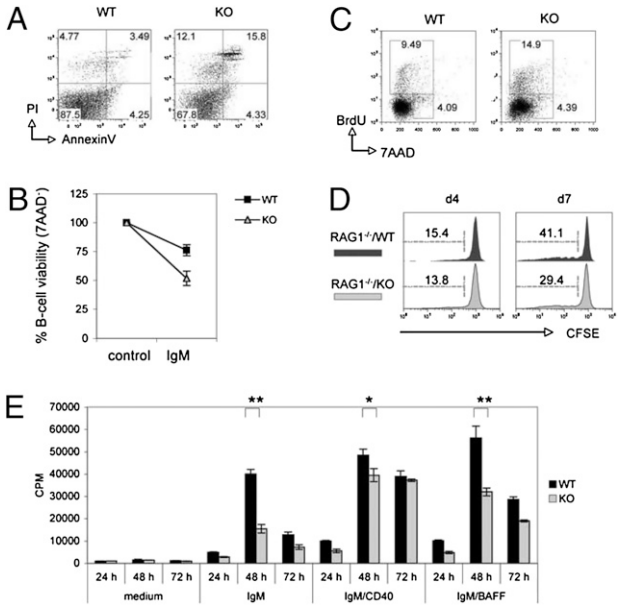

Fig. 2. B-cell apoptosis and proliferation. (*A*) Increased apoptosis of resting splenic B cells. FACS of PI versus Annexin V staining of $B220^+$-gated splenocytes. (*B*) Increased BCR-mediated apoptosis. Purified splenic B cells were left untreated (medium) or stimulated for 24 h with 5 μg/mL anti-IgM (IgM). Viability was determined by 7AAD staining and FACS. (*C*) Increased BrdU incorporation in vivo. WT and KO mice drank water containing 1 mg/mL BrdU for 3 d and $B220^+$ splenocytes were analyzed by intracellular staining and FACS (BrdU vs. 7AAD). (*D*) Inhibition of homeostatic expansion. Splenic B cells (5×10^6) were labeled with 5 μM CFSE and injected into 6-Gy–irradiated $RAG1^{-/-}$ mice. At 4 and 7 d after injection, $CD19^+$-gated splenocytes were analyzed by FACS. Data are the percentage of B cells showing CFSE decay relative to total B cells. (*E*) Reduced $[^3H]$thymidine incorporation. Splenic B cells (1×10^5) were left untreated (medium) or stimulated with 5 μg/mL anti-IgM (IgM), 5 μg/mL anti-IgM plus 5 μg/mL anti-CD40 (IgM/CD40), or 5 μg/mL anti-IgM plus 5 ng/mL BAFF (IgM/BAFF). $[^3H]$thymidine incorporation was assessed at 24, 48, or 72 h after seeding after a 9 h pulse (1 μCi). $*P < 0.05$; $**P < 0.005$.

To investigate the role of 14-3-3σ in lymphopenia-induced homeostatic proliferation, we performed adoptive transfer experiments in which carboxyfluorescein succinimidyl ester (CFSE)-labeled splenic B cells from WT or KO mice were i.v. injected into $RAG1^{-/-}$ mice. The percentage of B cells showing decayed CFSE fluorescence represents dividing B cells (22). At 4 d after injection, no significant differences were observed between $RAG1^{-/-}$/WT and $RAG1^{-/-}$/KO mice (Fig. 2*D*, *Left*). However, by day 7 after injection, KO B cells had clearly expanded less than WT B cells (Fig. 2*D*, *Right*). Thus, 14-3-3σ is required for B-cell homeostatic expansion.

Although loss of 14-3-3σ intensified BCR-mediated apoptosis (Fig. 2*B*), BCR engagement can also trigger B-cell activation and proliferation. We therefore determined whether 14-3-3σ deficiency impaired anti-IgM–stimulated B-cell proliferation. Splenic B cells from WT and KO mice were stimulated for 24, 48, or 72 h with soluble anti-IgM, with or without anti-CD40 or BAFF ligand, and proliferation was assessed by $[H^3]$thymidine incorporation. No differences were observed at 24 h but, by 48 h, $[^3H]$thymidine uptake by BCR-stimulated KO B cells was only approximately one third that of BCR-stimulated WT cells (Fig. 2*E*). Strikingly, this impairment was almost completely rescued by anti-CD40 treatment for 48 h, and no deficit existed by 72 h after stimulation with anti-IgM plus anti-CD40 (Fig. 2*E*). Curiously, this rescue effect was not replicated by anti-IgM plus BAFF stimulation. Thus, in addition to positively regulating BCR signaling, 14-3-3σ may negatively regulate CD40 signaling.

TD Immune Responses. Activated B cells up-regulate costimulatory molecules CD80 (B7.1) and CD86 (B7.2) as well as the activation marker CD25 (IL-2 receptor α) and CD69 (23). Expression of CD80 or CD86 enables activated B cells to interact with T cells and to receive signals inducing the germinal center (GC) formation necessary for the humoral response (24). We used FACS to examine whether 14-3-3σ was involved in BCR-induced up-regulation of CD80, CD86, CD25, and CD69. When WT and KO splenic B cells were stimulated with anti-IgM or anti-IgM plus anti-CD40, up-regulation of CD86 and CD25 on KO B cells was partially impaired, whereas CD69 and CD80 up-regulation was normal (Fig. S4). We then assessed the humoral response by injecting the TD immunogen 4-hydroxy-3-nitrophenylacetyl–chicken γ-globulin [$NP_{(15)}$-CG] into WT and KO mice. At 7, 14, and 21 d after injection, serum levels of anti-$NP_{(15)}$-CG–specific IgM and IgG_1 were determined by ELISA. In parallel, the induction of GC B cells ($B220^+PNA^+$) in the spleens of immunized WT and KO mice was examined on day 14 by IHC. Serum levels of anti-$NP_{(15)}$-CG–specific IgM and IgG_1 were comparable in WT and KO mice (Fig. 3 *A* and *B*). IHC analysis showed that PNA^+ GC was not detectable in WT mice before $NP_{(15)}$-CG immunization but were induced by day 14 after injection (Fig. 3*C*, *Top*). However, numerous spontaneous GCs were detectable in KO mice before immunization, with a further increase in GCs apparent by day 14 after injection (Fig. 3*C*, *Bottom*). Thus, loss of 14-3-3σ does not impair GC formation, or $NP_{(15)}$-CG–specific IgM production, or class-switch recombination (CSR) to $NP_{(15)}$-CG–specific IgG_1, indicating that 14-3-3σ is not a key player in BCR-mediated TD responses.

TI Immune Responses. We next assessed responses to TI immunogens in the absence of 14-3-3σ. We first injected TNP-Ficoll into WT and KO mice. ELISA of serum samples revealed a fourfold induction of TNP-specific IgM in WT mice by day 7 post-immunization but only a 1.5-fold increase in KO mice (Fig. 4*A*).

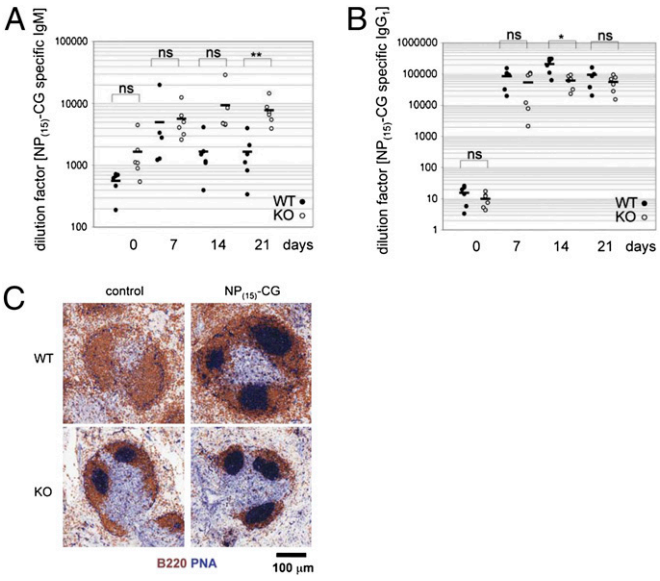

Fig. 3. TD immune responses. (*A* and *B*) Functional CSR. WT and KO mice ($n = 6$ per group) were i.p. injected with 100 μg $NP_{(15)}$-CG and serum levels of $NP_{(15)}$-CG–specific IgM (*A*) and IgG (*B*) were determined by ELISA on days 7, 14, or 21 after immunization. Day 0, preimmunization. Data are Ig titers of individual mice. Horizontal bars represent mean values ($*P < 0.05$; $**P < 0.005$; ns, not significant). (*C*) Increased spontaneous GC formation. WT and KO mice ($n = 3$ per group) were i.p. injected with 100 μg $NP_{(15)}$-CG. Before immunization (control), or on day 14 after immunization, spleen sections were stained with anti-B220 (brown) plus PNA (blue) to detect GCs.

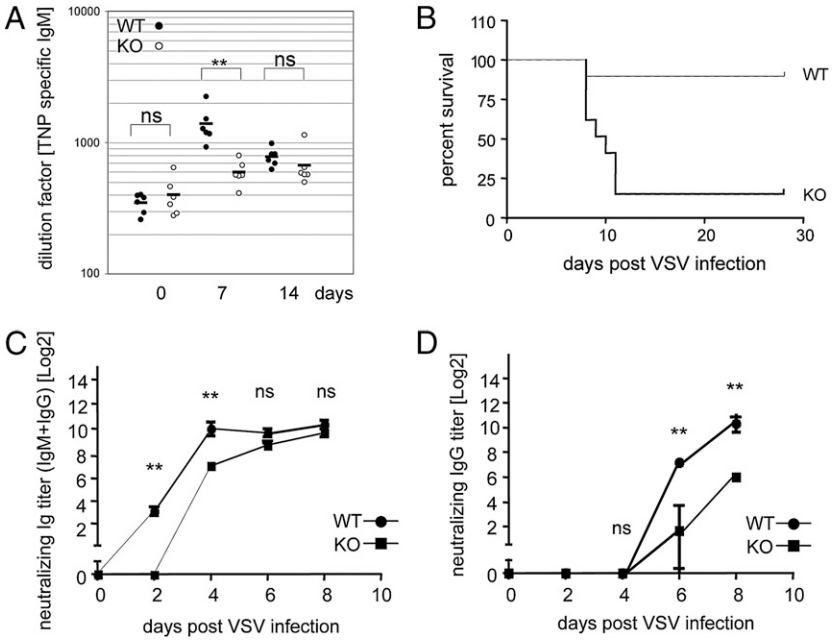

Fig. 4. TI immune responses. (*A*) Reduced TNP-specific IgM. WT and KO mice (n = 6 per group) were i.p. injected with 25 μg TNP-Ficoll. Serum samples were analyzed by ELISA on days 7 and 14 after immunization. Day 0, preimmunization. Data are Ig titers of individual mice. Horizontal bars indicate mean values. (*B*) Decreased resistance to VSV. WT and KO mice (n = 6 per group) were i.p. injected with 10^5 pfu VSV and viability was analyzed using Kaplan–Meier methodology. (*C* and *D*) Reduced anti-VSV neutralizing Abs. Serum samples from the mice in *B* were analyzed by ELISA on day 0 (preinfection) and on days 2, 4, 6, and 8 after infection to detect total anti-VSV IgM plus IgG (*C*) or VSV-specific IgG (*D*). $^{**}P < 0.005$; ns, not significant.

Nevertheless, loss of 14-3-3σ did not hamper TNP-specific CSR to IgG_3 in KO mice (Fig. S5*A*).

To examine immune responses to a more physiological TI immunogen, we infected WT and KO mice with vesicular stomatitis virus (VSV). Mice infected with VSV mount strong humoral and cellular TI responses in which IFN and neutralizing Ab play essential protective roles (25). The production of anti-VSV Ab requires that MZ B cells be activated via direct contact with a virus particle, a process independent of dendritic cells and T cells. MZ B cells activated in this way immediately secrete VSV-neutralizing IgM as an early response, and subsequently migrate to the T-cell zone of the spleen to participate in the induction of VSV-specific GC formation (26). We infected WT and KO mice with VSV and monitored survival and production of IFN-α and VSV-specific IgM and IgG_3. Surprisingly, seven of eight KO mice died between days 8 and 11 after infection, whereas only one of eight WT mice had died by this point (Fig. 4*B*). Examination of serum IFN-α production at 20 h after VSV immunization revealed equal production in WT and KO mice (Fig. S5*B*). Thus, mice lacking 14-3-3σ have a B-cell–intrinsic defect and decreased resistance to VSV challenge. The induction of total anti-VSV (IgM plus IgG) in WT mice was detectable by day 2 after infection, peaked on day 4, and remained high until day 8 (Fig. 4*C*). In contrast, total anti-VSV was undetectable in KO mice on day 2 after infection (Fig. 4*C*). However, by day 8 after infection, the mutants showed normal levels of total anti-VSV (Fig. 4*C*). When we specifically examined VSV-neutralizing IgG, WT mice first exhibited these Ab on day 6 after infection and their levels increased until day 8 after infection (Fig. 4*D*). However, in KO mice, anti-VSV IgG levels were only one third of controls on day 6 after infection and failed to achieve WT levels even by day 8 (Fig. 4*D*). Given the critical protective role of IgM during early VSV infection, the inability of KO mice to produce anti-VSV IgM by day 2 after infection likely led to their deaths.

FOXO Functions. 14-3-3 proteins regulate FOXOs transcription factors, which promote cellular survival by preventing apoptosis. To determine whether the elevated apoptosis of KO B cells was caused by dysregulated FOXO activity, we used qRT-PCR to compare mRNA levels of the FOXO target genes Bim (27), p21 (28), Mxi1 (29), and p27 (30). As expected, Bim and p21 mRNAs were induced approximately sevenfold in WT B cells treated for 6 h with anti-IgM plus CD40L (Fig. 5*A* and Fig. S6*A*). Strikingly, in KO B cells, these mRNAs, as well as Mxi mRNA, were induced by seven to 23 fold after 2 h of anti-IgM plus CD40L stimulation, and by seven to 15 fold after 6 h stimulation (Fig. 5*A* and Fig. S6 *A* and *B*). Curiously, p27 mRNA was suppressed in stimulated WT B cells but increased twofold after 6 h stimulation in KO B cells (Fig. S6*C*). Thus, FOXOs activity is aberrantly and selectively increased in the absence of 14-3-3σ.

Western blotting of the aforementioned cells revealed that protein levels of Bim and p27 were also up-regulated in resting KO B cells compared with WT (Fig. 5*B*). This observation implies that loss of 14-3-3σ in B cells elevates FOXO activity, which in turn increases Bim protein and thus spontaneous apoptosis. However, FOXO1 protein was strongly reduced in KO B cells (Fig. 5*B*), although FOXO1 mRNA levels were normal (Fig. 5*C*). Importantly, treatment of KO B cells with the proteasome inhibitor MG132 efficiently restored normal FOXO1 protein (Fig. 5*D*), indicating that the decreased FOXO1 protein in KO B cells was a result of enhanced FOXO1 degradation.

Based on the known interaction of 14-3-3ζ with FOXO3a (12, 17), we investigated whether 14-3-3σ regulated FOXO1 via direct protein–protein interaction. Overexpression of His-tagged 14-3-3σ and Flag-tagged FOXO1 in 293T cells showed that these two molecules could indeed associate (Fig. 5*E*). We then used anti–14-3-3σ and anti-FOXO1 to examine the association between endogenous FOXO1 and 14-3-3σ in the Ramos human B-cell line and found that anti–14-3-3σ could coimmunoprecipitate endogenous FOXO1 (Fig. 5*F*). Moreover, upon BCR stimulation via anti-IgM, increased FOXO1 protein associated with 14-3-3σ but only in the cytosolic fraction of Ramos cells (Fig. 5*F*). No interaction between 14-3-3σ and FOXO1 proteins was detected in the nuclei of stimulated Ramos cells. These results suggest that 14-3-3σ can interact with and protect FOXO1 protein from degradation in the cytoplasm, but that the effects of 14-3-3σ on FOXO activity are indirect.

Constitutively active FOXO4 suppresses Akt activity (31), and overexpression of the human FOXO1 S256A mutant protein, which blocks 14-3-3 protein binding, inhibits Akt activation (32). Thus, a feedback loop may exist between FOXO and Akt in which increased FOXO activity, or loss of the 14-3-3 protein binding site on FOXO, leads to impaired Akt activation. When we stimulated KO B cells with anti-IgM, both P-Akt and P-Erk1/2 were dramatically decreased (Fig. 5*G*). This signaling deficit

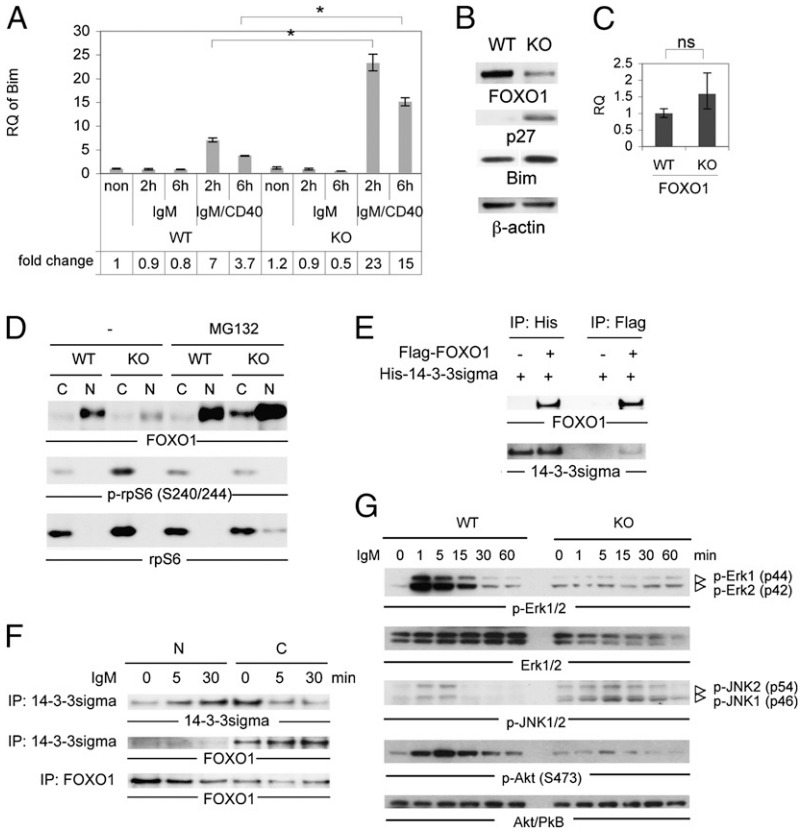

Fig. 5. FOXO functions. (*A*) Increased FOXO target gene (Bim) mRNA. Splenic B cells were left untreated (non) or stimulated for 2 or 6 h with 10 μg/mL anti-IgM or 10 μg/mL anti-IgM plus 1 μg/mL CD40L (IgM/CD40). Bim mRNA was determined by qRT-PCR. Data are Bim mRNA relative to 18S RNA. ΔΔCt values were normalized to WT values in untreated controls (fold change, 1). $*P < 0.05$. (*B*) Altered proteins. Western blot of FOXO1, p27, Bim, and β-actin proteins in resting WT and KO B cells. (*C*) Normal FOXO1 mRNA. qRT-PCR of FOXO1 mRNA in resting WT and KO B cells. (*D*) Restoration of FOXO1 protein by proteasome inhibition. Purified WT and KO B cells were left untreated (–) or treated with MG132 (20 μM) for 1 h at 37 °C. Nuclear (N) and cytosolic (C) fractions of cells were immunoblotted to detect FOXO1 protein, P-S6 ribosomal protein (Ser240/244; p-rpS6), and total S6 ribosomal protein (rpS6; loading control for cytosol). (*E*) FOXO1 interacts directly with 14-3-3σ protein under overexpression conditions. 293T cells were transiently transfected with plasmid encoding His-tagged 14-3-3σ, without (–) or with (+) plasmid encoding Flag-tagged FOXO1. At 2 d after transfection, total lysates were immunoprecipitated with beads conjugated to anti-His (IP: His) or anti-Flag (IP: Flag) and immunoblotted to detect FOXO1 and 14-3-3σ. (*F*) FOXO1 interacts directly with endogenous 14-3-3σ in the cytosol. Ramos B cells were left untreated (0) or stimulated with anti-human IgM for 5 or 30 min. Nuclear (N) and cytosolic (C) fractions of cells were immunoprecipitated with anti–14-3-3σ or anti-FOXO1 and immunoblotted to detect 14-3-3σ and FOXO1. (*G*) Altered signaling downstream of BCR engagement. Purified WT and KO B cells were left untreated (0) or stimulated with 10 μg/mL anti-IgM for the indicated times. Lysates were immunoblotted to detect P-Erk1/2, total Erk1/2, P-JNK1/2, P-Akt (S473), and total Akt.

resembles the defect in B cells lacking FOXO1 (15), suggesting that both 14-3-3σ and FOXO1 are required for optimal signaling downstream of BCR engagement. However, unlike FOXO1-deficient B cells, 14-3-3σ–deficient B cells undergo massive apoptosis upon BCR stimulation. This difference may stem from the residual FOXO1 activity that persists in the absence of 14-3-3σ and presumably drives B-cell apoptosis.

Discussion

This study of 14-3-3σ–deficient mice has demonstrated the critical role of 14-3-3σ in B-cell biology. Loss of 14-3-3σ increases the apoptosis of peripheral B cells, disrupting B-cell homeostasis. It is attributable to the impaired BCR signaling that also hampers BCR-mediated proliferation and TI B-cell responses. Although KO B cells showed enhanced proliferation in vivo, adoptive transfer in RAG1$^{-/-}$ mice revealed that KO B cells failed to undergo homeostatic expansion efficiently in lymphopenia host. We thus speculate that the enhanced proliferation of KO B cells in vivo is an attempt to compensate for the increased apoptotic loss of B cells. We showed that the drastic apoptosis in KO B cells is correlated with increased FOXO activity and elevated Bim. In addition, 14-3-3σ interacts with FOXO1 in the cytoplasm and protects it from proteasome-dependent degradation. Although FOXO3a plays a role in peripheral B-cell maintenance (16), whether 14-3-3σ regulates B-cell survival via preservation of FOXO3a requires further investigation. Our findings indicate that 14-3-3σ is essential for the maintenance of FOXO1 at a consistent level that supports B-cell survival.

The increased apoptosis in KO B cells is possibly not only caused by the activation of FOXO/Bim pathway, but also a perturbation of prosurvival/proapoptosis regulation. IgM/CD40 stimulation of KO B cells for 2 h results in a twofold increase in Bcl-6 mRNA, whereas the same treatment of WT B cells reduces Bcl-6 (Fig. S7*A*). As induction of Bcl-6 mediated by FOXO can down-regulate prosurvival gene *Bcl-xL* (33), the aberrant FOXO activity that results from loss of 14-3-3σ may lead to a disorderly pattern of prosurvival/proapoptosis gene expression that consequently impair B-cell survival. Because no interaction between endogenous 14-3-3σ and FOXO1 is detected in B-cell nuclei, one possibility will be that 14-3-3σ inhibits FOXO activity indirectly via the abnormal BCR signaling cascade that essentially alters the posttranslation modification of FOXO (34). We found that BCR stimulation in KO B cells could not induce the maximal FOXO1 S256 phosphorylation at 5 min after BCR stimulation as in WT (Fig. S7*B*); this is the residue phosphorylated by Akt that mediates 14-3-3 binding (17, 18). It indicates that FOXO1 of reduced S256 phosphorylation status caused by loss of 14-3-3σ cannot be efficiently sequestered in the cytoplasma upon BCR stimulation, which will promote FOXO1 activity.

The PI3K/Akt/FOXO pathway is critical for B-cell development and survival (9–11, 35). As 14-3-3σ is dispensable for early B-cell development, an alternative mechanism whose function is analogous to that of 14-3-3σ may modulate FOXO in B-cell progenitors. Our preliminary work reveals that 14-3-3ε and 14-3-3η mRNAs are highly expressed in B220^{+}IgM^{-} B-cell progenitors (Fig. S7*C*). It is thus possible that different 14-3-3 proteins perform parallel functions at different stages of B-cell development. Attenuation of PI3K/Akt pathway is also necessary for B-cell function, which enhances AID expression and accelerates CSR (15, 36). Thereby, the reduced Akt activation in BCR-stimulated KO B cells may explain why increased TNP-specific IgG3 is observed in resting KO mice (Fig. S5*A*).

Loss of 14-3-3σ leads to a strikingly impaired TI immune response in KO mice. The mutant B cells failed to produce VSV-specific neutralizing IgM by day 2 after challenge, a defect likely cause by their severely reduced MZ B-cell numbers and the impaired BCR signaling in these cells. Surprisingly, despite the reduced CD86/CD25 expression upon IgM stimulation in vitro, KO mice exhibited functional TD immune responses. Thus, loss of 14-3-3σ does not block the interaction between activated B cells

and T cells in vivo. Because IgM/CD40 stimulation caused KO B cells to proliferate almost as well as WT B cells by 48 h, and just as well by 72 h, the functional TD responses observed in KO mice may be driven by CD40L–CD40 signaling that compensates for the deficit in BCR signaling. As IgM/CD40 stimulation in KO B cells failed to reduce apoptosis to WT level (WT, 5.32%; KO, 17%), we speculate that IgM/CD40 signaling provides additional signals for proliferation, rather than preventing KO B cell from apoptosis (Fig. S8*A*). Consistent with this idea, IgM/CD40 stimulation did not induce increased amount of Bim protein in KO B cells, although significant amount of Bim mRNA was induced (Fig. 5*A* and Fig. S8*B*). Furthermore, Akt S473 phosphorylation mediated by IgM/CD40 stimulation in KO B cells completely overrode WT level, whereas Erk phosporylation did not (Fig. S8 *C* and *D*). Thus, 14-3-3σ may negatively regulate B-cell proliferation via AKT upon IgM/CD40 stimulation. In preliminary work, we have noted that LPS-stimulated KO B cells display enhanced proliferation and differentiate more rapidly into IgG_3^+ plasmablasts (Fig. S7 *D* and *E*). Thus, such a role in CD40 or TLR4 signaling could account for the elevated spontaneous GC formation observed in KO mice. Taken together, our results implicate 14-3-3σ as a crucial multifaceted regulator of the immune system.

Materials and Methods

14-3-3σ–deficient mice were generated by conventional gene targeting (37). For adoptive transfer, RAG1$^{-/-}$ or μMT mice were γ-irradiated (6 Gy) and 5×10^6 BM cells were i.v. injected. At 8 wk after transfer, B cells were analyzed by FACS. For B-cell purification, splenocytes were incubated with specific Ab and streptavidin beads (Becton Dickinson). Non-B cells were depleted using the BD IMag Cell Separation Magnet system. Purity was greater than 94%. Homeostatic expansion in RAG1$^{-/-}$ mice was assessed by CFSE decay (22). For TI and TD responses, mice were i.p. immunized with 25 μg TNP-Ficoll (TI) or 100 μg $NP_{(15)}$-CG (TD). Serum samples for day 0 (preimmunization) and days 7 and 21 after immunization were analyzed by ELISA. For qRT-PCR, splenic B cells (10^7) were stimulated with 10 μg/mL anti-IgM (Southern Biotech) for 2 or 6 h, with or without 1 μg/mL CD40L (PeproTech). cDNA was produced from 500 ng RNA (RNeasy kit; Qiagen) and SuperScript III (Invitrogen). Primers are listed in *SI Materials and Methods*. cDNAs were amplified using SYBR Green (model 7900; Applied Biosystems). The gene-specific fold change, normalized to 18S RNA, was calculated using the $2^{-\Delta\Delta ct}$ method by comparison with untreated WT (38). For nuclear/cytosolic fractionation, B cells (1×10^7) were lysed in Nonidet P-40 buffer and nuclei were pelleted by centrifugation at 15,000 rpm (Eppendorf, centrifuge 5417R, Rotor F-45-30-11) for 2 min at 4 °C. For nuclear fractions, buffer C (*SI Materials and Methods*) was added to the pellet followed by centrifugation at 15,000 rpm for 10 min at 4 °C. For proteasome studies, B cells (1×10^7) were treated with proteasome inhibitor MG132 (20 μM; Calbiochem) for 1 h at 37 °C, followed by nuclear/cytosolic fractionation. For VSV challenge, mice were i.v. injected with 2×10^6 pfu VSV-Indiana (39) and serum samples were collected on days 0, 2, 4, 6, and 8. VSV-specific neutralization assay has been carried out as previously described (40). Serum immunoglobulins were measured by ELISA. ELISA, FACS, IHC, BrdU, thymidine incorporation, and Western blotting, performed by using standard protocols. *SI Materials and Methods* provides further details.

ACKNOWLEDGMENTS. We thank Dr. H. You, Dr. B. Vogelstein, and Dr. H. Hermeking for reagents and discussion, and M. Saunders for scientific editing. Y.-W.S. is a recipient of a postdoctoral fellowship from the Cancer Research Institute, New York, NY.

1. Fu H, Subramanian RR, Masters SC (2000) 14-3-3 proteins: Structure, function, and regulation. *Annu Rev Pharmacol Toxicol* 40:617–647.
2. Muslin AJ, Tanner JW, Allen PM, Shaw AS (1996) Interaction of 14-3-3 with signaling proteins is mediated by the recognition of phosphoserine. *Cell* 84:889–897.
3. Yaffe MB, et al. (1997) The structural basis for 14-3-3:phosphopeptide binding specificity. *Cell* 91:961–971.
4. Obsilová V, Silhan J, Boura E, Teisinger J, Obsil T (2008) 14-3-3 proteins: A family of versatile molecular regulators. *Physiol Res* 57(Suppl 3):S11–S21.
5. Hermeking H, et al. (1997) 14-3-3 sigma is a p53-regulated inhibitor of G2/M progression. *Mol Cell* 1:3–11.
6. Chan TA, Hermeking H, Lengauer C, Kinzler KW, Vogelstein B (1999) 14-3-3Sigma is required to prevent mitotic catastrophe after DNA damage. *Nature* 401:616–620.
7. Wilker EW, et al. (2007) 14-3-3sigma controls mitotic translation to facilitate cytokinesis. *Nature* 446:329–332.
8. Martin F, Kearney JF (2000) B-cell subsets and the mature preimmune repertoire. Marginal zone and B1 B cells as part of a "natural immune memory". *Immunol Rev* 175:70–79.
9. Lam KP, Kühn R, Rajewsky K (1997) In vivo ablation of surface immunoglobulin on mature B cells by inducible gene targeting results in rapid cell death. *Cell* 90: 1073–1083.
10. Torres RM, Flaswinkel H, Reth M, Rajewsky K (1996) Aberrant B cell development and immune response in mice with a compromised BCR complex. *Science* 272:1804–1808.
11. Werner M, Hobeika E, Jumaa H (2010) Role of PI3K in the generation and survival of B cells. *Immunol Rev* 237:55–71.
12. Brunet A, et al. (1999) Akt promotes cell survival by phosphorylating and inhibiting a Forkhead transcription factor. *Cell* 96:857–868.
13. Burgering BM, Medema RH (2003) Decisions on life and death: FOXO Forkhead transcription factors are in command when PKB/Akt is off duty. *J Leukoc Biol* 73: 689–701.
14. Greer EL, Brunet A (2005) FOXO transcription factors at the interface between longevity and tumor suppression. *Oncogene* 24:7410–7425.
15. Dengler HS, et al. (2008) Distinct functions for the transcription factor Foxo1 at various stages of B cell differentiation. *Nat Immunol* 9:1388–1398.
16. Hinman RM, et al. (2009) Foxo3-/- mice demonstrate reduced numbers of pre-B and recirculating B cells but normal splenic B cell sub-population distribution. *Int Immunol* 21:831–842.
17. Brunet A, et al. (2002) 14-3-3 transits to the nucleus and participates in dynamic nucleocytoplasmic transport. *J Cell Biol* 156:817–828.
18. Van Der Heide LP, Hoekman MF, Smidt MP (2004) The ins and outs of FoxO shuttling: Mechanisms of FoxO translocation and transcriptional regulation. *Biochem J* 380: 297–309.
19. Yuan Z, et al. (2009) Regulation of neuronal cell death by MST1-FOXO1 signaling. *J Biol Chem* 284:11285–11292.
20. Dong S, et al. (2007) 14-3-3 Integrates prosurvival signals mediated by the AKT and MAPK pathways in ZNF198-FGFR1-transformed hematopoietic cells. *Blood* 110: 360–369.
21. Tsubata T, Wu J, Honjo T (1993) B-cell apoptosis induced by antigen receptor crosslinking is blocked by a T-cell signal through CD40. *Nature* 364:645–648.
22. Lyons AB, Parish CR (1994) Determination of lymphocyte division by flow cytometry. *J Immunol Methods* 171:131–137.
23. Wong SC, et al. (2002) Peritoneal CD5+ B-1 cells have signaling properties similar to tolerant B cells. *J Biol Chem* 277:30707–30715.
24. Borriello F, et al. (1997) B7-1 and B7-2 have overlapping, critical roles in immunoglobulin class switching and germinal center formation. *Immunity* 6:303–313.
25. Steinhoff U, et al. (1995) Antiviral protection by vesicular stomatitis virus-specific antibodies in alpha/beta interferon receptor-deficient mice. *J Virol* 69:2153–2158.
26. Scandella E, et al. (2007) Dendritic cell-independent B cell activation during acute virus infection: A role for early CCR7-driven B-T helper cell collaboration. *J Immunol* 178:1468–1476.
27. Dijkers PF, Medema RH, Lammers JW, Koenderman L, Coffer PJ (2000) Expression of the pro-apoptotic Bcl-2 family member Bim is regulated by the forkhead transcription factor FKHR-L1. *Curr Biol* 10:1201–1204.
28. Hawke TJ, Jiang N, Garry DJ (2003) Absence of p21CIP rescues myogenic progenitor cell proliferative and regenerative capacity in Foxk1 null mice. *J Biol Chem* 278: 4015–4020.
29. Delpuech O, et al. (2007) Induction of Mxi1-SR alpha by FOXO3a contributes to repression of Myc-dependent gene expression. *Mol Cell Biol* 27:4917–4930.
30. Medema RH, Kops GJ, Bos JL, Burgering BM (2000) AFX-like Forkhead transcription factors mediate cell-cycle regulation by Ras and PKB through p27kip1. *Nature* 404: 782–787.
31. Yang H, Zhao R, Yang HY, Lee MH (2005) Constitutively active FOXO4 inhibits Akt activity, regulates p27 Kip1 stability, and suppresses HER2-mediated tumorigenicity. *Oncogene* 24:1924–1935.
32. Rena G, Prescott AR, Guo S, Cohen P, Unterman TG (2001) Roles of the forkhead in rhabdomyosarcoma (FKHR) phosphorylation sites in regulating 14-3-3 binding, transactivation and nuclear targetting. *Biochem J* 354:605–612.
33. Calnan DR, Brunet A (2008) The FoxO code. *Oncogene* 27:2276–2288.
34. Tang TT, et al. (2002) The forkhead transcription factor AFX activates apoptosis by induction of the BCL-6 transcriptional repressor. *J Biol Chem* 277:14255–14265.
35. Srinivasan L, et al. (2009) PI3 kinase signals BCR-dependent mature B cell survival. *Cell* 139:573–586.
36. Omori SA, et al. (2006) Regulation of class-switch recombination and plasma cell differentiation by phosphatidylinositol 3-kinase signaling. *Immunity* 25:545–557.
37. Torres R, Kuehn R (1997) *Laboratory Protocols for Conditional Gene Targeting* (Oxford University Press, Oxford, UK).
38. Livak KJ, Schmittgen TD (2001) Analysis of relative gene expression data using real-time quantitative PCR and the 2(-Delta Delta C(T)) method. *Methods* 25:402–408.
39. Charan S, Zinkernagel RM (1986) Antibody mediated suppression of secondary IgM response in nude mice against vesicular stomatitis virus. *J Immunol* 136:3057–3061.
40. Junt T, et al. (2002) Antiviral immune responses in the absence of organized lymphoid T cell zones in plt/plt mice. *J Immunol* 168:6032–6040.